

Structural characterization of H plasma-doped ZnO single crystals by positron annihilation spectroscopies

Wolfgang Anwand^{*1}, Gerhard Brauer¹, Thomas E. Cowan¹, Dieter Grambole², Wolfgang Skorupa², Jakub Čížek³, Jan Kuriplach³, Ivan Procházka³, Werner Egger⁴, and Peter Sperr⁴

¹Institut für Strahlenphysik, Forschungszentrum Dresden-Rossendorf, P.O. Box 510 119, 01314 Dresden, Germany

²Institut für Ionenstrahlphysik und Materialforschung, Forschungszentrum Dresden-Rossendorf, P.O. Box 510 119, 01314 Dresden, Germany

³Department of Low Temperature Physics, Charles University, V Holešovičkách 2, 18000 Prague, Czech Republic

⁴Institut für Angewandte Physik und Messtechnik, Fakultät für Luft- und Raumfahrttechnik, Universität der Bundeswehr, Heisenbergweg 39, 85579 Neubiberg, Germany

Received 3 December 2009, revised 2 July 2010, accepted 7 July 2010

Published online 24 August 2010

Keywords defects, doping, positron annihilation, vacancies, ZnO

* Corresponding author: e-mail w.anwand@fzd.de, Phone: +49 351 260 2117, Fax: +49 351 260 12117

Nominally undoped, hydrothermally grown ZnO single crystals have been investigated before and after exposure to remote H plasma. Structural characterizations have been made by various positron annihilation spectroscopies (continuous and pulsed slow positron beams, conventional lifetime). The content of bound hydrogen (H-b) before and after the remote

H plasma treatment at the polished side of the crystals was determined at depths of 100 and 600 nm, respectively, using nuclear reaction analysis. At a depth of 100 nm, H-b increased from (11.8 ± 2.5) to $(48.7 \pm 7.6) \times 10^{19} \text{ cm}^{-3}$ after remote H plasma treatment, whereas at 600 nm no change in H-b was observed.

© 2010 WILEY-VCH Verlag GmbH & Co. KGaA, Weinheim

1 Introduction Unresolved controversies in research on the properties of ZnO are mainly related to native defects formed during crystal growth. Very recently a systematic study of various, nominally undoped ZnO single crystals, either hydrothermally grown (HTG) or melt grown (MG), has been performed [1]. A single positron lifetime (LT) was observed in all crystals investigated, which clustered at 180–182 and 165–167 ps for HTG and MG crystals, respectively. Furthermore, hydrogen – hereafter referred to as H – was detected in all crystals in a bound state with a high concentration (at least 0.3 at.-%), whereas the concentrations of other impurities are very small. *Ab initio* calculations suggest the existence of Zn vacancy-H complexes. However, the role of H in ZnO is still far from being completely understood.

Di-vacancy-H complexes have been considered in a further recent study [2].

In another recent paper, various defect studies of (0001) oriented HTG ZnO crystals electrochemically doped with H were presented [3]. The H content in the crystals was

determined by nuclear reaction analysis (NRA) and found to be in reasonable agreement with concentrations calculated from Faraday's law. A single positron LT of 182 ps was measured in the virgin crystals and attributed to saturated positron trapping at Zn vacancies surrounded by H atoms, which exist at 0.3 at.-% in the crystals. It was further demonstrated that up to ~30 at.-% H can be introduced into the crystals by electrochemical doping. More than half of this amount has been estimated to be chemically bound, i.e., incorporated into the ZnO crystal lattice. However, this drastic increase of the H concentration was found to be of marginal impact on the measured positron LT, whereas a contribution from positrons annihilated by electrons which belong to O–H bonds formed in the H doped crystal is clearly seen in coincidence Doppler broadening (CDB) spectra. In addition, the formation of hexagonally shaped pyramids on the surface of the H doped crystals has been observed by optical microscopy.

In general, H-related defects have attracted significant attention recently because of their potential for tailoring ZnO

© 2010 WILEY-VCH Verlag GmbH & Co. KGaA, Weinheim

properties. Remote plasma processing has been used to achieve H doping for photoluminescence (PL) studies [4–6]. Already from these few papers and references therein it may be seen that there is substantial experimental evidence that H affects ZnO in several ways, including the modification of electrical and optoelectronic properties, and the passivation of deep levels. However, no quantitative estimates of H doping levels achieved by plasma processing are given, and final conclusions cannot be drawn regarding the structure of the defects to which H is related.

In the authors' opinion an estimation of the true H content of the ZnO materials under investigation is absolutely necessary in order to check and maybe support existing ideas from theory [7, 8] about its possible role in the ZnO lattice. Generally it is seen that studies in which H detection is performed by secondary ion mass spectroscopy (SIMS) do not touch upon the sensitivity and background level of H during SIMS analysis, as they focus on H depth profiling. Furthermore, it is common practice to calibrate SIMS measurements either by NRA or by well-defined standards produced by ion implantation of H into a given material [9, 10]. However, this seems to be impractical in the case of ZnO simply because the initial H concentration has been found to be already very large [1, 3]. Therefore, NRA is the method of choice in this work to characterize the effect of H plasma doping.

Positron annihilation spectroscopy (PAS) [11–14] is now a well-established tool for the study of electronic and defect properties of bulk solids and thin films. It has been applied in this work in the form of conventional positron LT measurements, a continuous beam of mono-energetic positrons (SPIS), and a pulsed low energy positron beam system (PLEPS) to characterize HTG ZnO single crystals exposed to remote H plasma.

The paper is organized as follows: in Section 2 experimental details are given, and in Section 3 the experimental results are presented and discussed. Conclusions are drawn in Section 4.

2 Experimental

2.1 Sample description Ten HTG single crystals typically of dimensions $10 \times 10 \times 0.5 \text{ mm}^3$ were supplied in 2008 by MaTecK GmbH (Jülich) (MT-08), with their O-face polished. A HTG sample bought in 2004 (MT-04) has been studied previously [15].

The ten, consecutively numbered MT-08 samples, formed five pairs (1/2, 3/4, 5/6, 7/8, and 9/10) which have been first characterized by LT measurements. Then, by assuming that all samples are nominally equal, sample #1

was cut to obtain a pair of $5 \times 7 \text{ mm}^2$ for LT and CDB measurements, and a remaining $10 \times 3 \text{ mm}^2$ part has been used for an estimation of the chemical composition in its virgin state. The H content and PAS studies (LT, CDB) before and after remote H plasma loading have been performed on the $5 \times 7 \text{ mm}^2$ sample pair. The CDB results will be published elsewhere.

Samples #2 and #3 were arbitrarily chosen for a more comprehensive investigation by SPIS and atomic force microscopy (AFM) before and after remote H plasma loading under the same conditions as sample #1. The AFM results will be published elsewhere.

The chemical compositions of arbitrarily chosen samples #1 and #5 were estimated by inductively coupled-plasma mass-spectrometry (ICP-MS) using a Perkin-Elmer ELAN-9000 spectrometer, with results given in Table 1. The relation between the atomic (C_{at}) concentrations estimated by ICP-MS and the volume (C_{vol}) concentrations in Table 1 are given by: $C_{\text{vol}} = C_{\text{at}}/\Omega$, where Ω is the volume per atom. According to the ZnO lattice parameters [16] used in previous calculations [17], $\Omega = 11.91 \times 10^{-24} \text{ cm}^3$.

2.2 H content and plasma doping The H content was determined by NRA [18] using 6.64 MeV ^{15}N ions, as successfully demonstrated earlier for HTG ZnO nanorods [19]. Our NRA has a depth resolution of $\sim 5 \text{ nm}$, and the H detection limit is $\sim 200 \text{ ppm}$. The chosen depth for the analysis is estimated by SRIM (“The Stopping and Range of Ions in Matter” – software which describes the transport properties of ions in matter [20]) calculations.

From SRIM it is also found that the analyzing ^{15}N ions lose their kinetic energy E with increasing penetration depth x mainly by electronic stopping ($(dE/dx)_{\text{electronic}} = 2.52 \text{ keV nm}^{-1}$), whereas nuclear stopping is about two orders of magnitude smaller ($(dE/dx)_{\text{nuclear}} = 0.006 \text{ keV nm}^{-1}$). This energy transfer to the crystal during analysis can be sufficient to release a weakly bound H atom from its bonding site, so that it will be able to start diffusion. It is generally assumed that single H atoms would be trapped again immediately, so that this diffusion should most probably involve H_2 molecules. As this diffusing H is then no longer available at the analysis position, this is seen as a drop in concentration with increasing ^{15}N fluence. Throughout this paper we will call this “unbound H (H-u)”. All H atoms which are not moving during analysis because the energy transfer is not sufficient to release them from their bonding site will be called “bound H (H-b)”. However, it has to be clearly stated also that from NRA it is impossible to draw any conclusion on the kind of bonding of H atoms in the crystal.

Table 1 Chemical composition (volume concentration, in 10^{17} cm^{-3} units) estimated for two HTG ZnO single crystals (MT-08, samples #1 and #5).

	Li	Mg	Ni	Cu	Ga	Rb	Mo	Ag	Cd	Te	Ba	Pb
no. 1	4.06	1.84	0.65	1.10	0.76	0.02	0.02	0.12	0.33	0.12	0.10	0.02
no. 5				1.03	1.55	0.02	0.06	0.34	0.45		0.25	0.08

The samples have been exposed for 1 h to a remote H dc plasma in a parallel-plate system, with a plate voltage of 1000 V. Samples were mounted on a heater block held at a temperature of 350 °C placed \sim 100 mm downstream from the plasma with a bias voltage of approximately -330 V, which fixed the bias current to ~ 50 μ A. During the loading the gas pressure was held at ~ 1 mbar.

2.3 PAS SPIS measurements were carried out with the mono-energetic positron beam “SPONSOR” at Rossendorf [21] at which a variation of the positron energy E from 30 eV to 36 keV with a smallest step width of 50 eV, if required, is possible. The energy resolution of the Ge detector at 511 keV is (1.09 ± 0.01) keV, resulting in a high sensitivity to changes in material properties from surface to depth. About 10^6 events per spectrum were accumulated.

The momentum of the electron–positron pair prior to annihilation causes Doppler broadening of the 511 keV annihilation line and can be characterized by the line-shape parameters S and W . The usefulness of these parameters may be illustrated further by an S – W plot, which allows one to conclude whether the changes are due to a change in concentration or type of a defect. For a more general discussion of these parameters we refer to the literature [11, 12]. In brief, the value of S is defined by the ratio of counts in the central region of the annihilation gamma peak to the total number of counts in the peak. It is common to define the central region for a certain sample to obtain $S \sim 0.5$ for the ZnO reference sample. The value of W is defined as the ratio of counts in the high-momentum regions symmetrical to the peak and the total number of counts so that here $W \sim 0.09$ for the ZnO reference sample. The same regions are then used to calculate the values of S and W for every other sample studied [12].

The bulk of a virgin MG ZnO specimen (see Ref. [17]) served as reference with $S \sim 0.5$ and $W \sim 0.09$. The depth information was obtained from the correlation of S and W with positron energy E using the versatile program package VEPFIT [22], in which a density of 5.605 g cm $^{-3}$ for ZnO was used. A mean positron penetration depth $\langle z \rangle$ (in nm) is calculated by the formula $\langle z \rangle = (A/\rho) \times E^{1.62}$, with ρ being the crystal density (in g cm $^{-3}$), E the positron energy (in keV), and A a material dependent parameter [22]. In Ref. [22], a value $A = 40$ is given. However, from our long-time experience in using VEPFIT it was found that a value $A = 36$ fits much better to a wide range of materials including ZnO.

The PLEPS system originally based on positrons from a radioactive source [14] has now been installed at the high intensity positron source (NEPOMUC) at the Munich Research Reactor FRM-II. In order to enhance the performance of the system, several improvements have been installed [23, 24]. The latest version of the PLEPS system has been used to perform depth-dependent positron LT measurements after remote H plasma loading of the ZnO crystals. For each incident positron energy E in the range 0.5–18 keV about $(4\text{--}6) \times 10^6$ events were collected per spectrum.

A $^{22}\text{NaCl}$ positron source (~ 1.5 MBq) deposited on a 2 μ m thick Mylar foil was used in LT and CDB measurements. This source was always covered with two identically treated ZnO crystals thus forming a sandwich. The depth profile of the positrons in each sample exhibits a distribution which reaches a maximum at ~ 43 μ m and has a low intensity tail that extends as deep as ~ 173 μ m into ZnO [25]. It has been estimated [3] that $\sim 90\%$ of the positrons are annihilated within 100 μ m of the surface, i.e., about 1/5 of the sample thickness. Therefore, the volume fraction sampled with the low energy positrons during SPIS and PLEPS measurements is a negligible part of the volume sampled with beta positrons during LT and CDB measurements, and that completely different parts of a sample are investigated depending on the methods used.

All LT measurements were performed at room temperature (RT) by a fast-fast spectrometer having a timing resolution of 160 ps [26] (FWHM ^{22}Na), and collecting $\sim 4 \times 10^7$ events per spectrum. The positron source contribution in the LT spectra consisted of two weak components with LTs of ~ 368 ps and ~ 1.5 ns, and corresponding intensities of ~ 8 and $\sim 1\%$, respectively. Each LT spectrum was decomposed using a maximum likelihood procedure described in detail elsewhere [27].

3 Results and discussion

3.1 PAS–SPIS and PLEPS SPIS results of the virgin MT-08 crystals are presented and compared in Fig. 1.

There is a Makhovian depth profile which corresponds to each positron energy which represents the initial distribution of positrons inside the material; this has been used to compute the mean depths shown on the upper axes in Figs. 1–3. However, following implantation the positrons

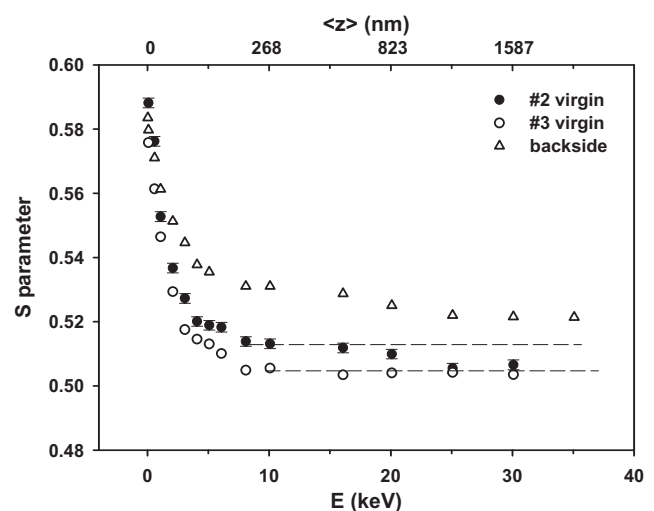


Figure 1 Doppler broadening parameter S of HTG ZnO single crystals (MT-08) as a function of incident positron energy E in as-received state (polished front side) and for a backside. The bulk S level of sample #3 and the defect level of the wider subsurface layer in sample #2 (see text) are indicated by lines to guide the eye. The mean positron implantation depth $\langle z \rangle$ is given for comparison.

will diffuse inside the material until they undergo annihilation from a free or trapped state. Therefore, only by comprehensive analysis using the VEPFIT programme package [22] it is possible to arrive at reliable parameters describing the positron behavior in any material. This has been done and the results are discussed below.

In both crystals, the existence of a narrow defected subsurface layer of ~ 100 nm thickness is indicated. In addition, sample #2 contains a further defected layer of (634 ± 141) nm width, and both layers have a positron diffusion length of $L_+ < 10$ nm. Compared to the previously investigated crystal MT-04 [15], where no such defected layers at the polished side have been observed, this indicates a varying quality of crystal polishing from the same supplier. However, the crystal quality can be characterized in terms of the bulk diffusion length, which was found to increase slightly from $L_+ = (22 \pm 1)$ nm for the MT-04 sample [15] to $L_+ = (38 \pm 11)$ nm for the MT-08 samples.

SPIS results typical of the unpolished backside of the MT-08 samples are presented in Fig. 1 for comparison and point to the presence of an increased damage level reaching deeper than ~ 4 μ m.

The existence of such defected layers and the surface roughness (observable by AFM) explain why as-received ZnO wafers are often found insufficient for epitaxial growth [28, 29]. However, it has been shown that thermal treatment can remove the damaged surface layer, thus allowing homoepitaxial growth of high-quality thin films [28, 29].

SPIS results for sample #2 after remote H plasma treatment are presented in Fig. 2.

The $S(E)$ curve shows three plateaus leading to the assumption that a three layer fit has to be used for the VEPFIT procedure. However, a three layer model resulted in a totally

unrealistic positron diffusion length of more than 500 nm for bulk ZnO. Consequently, it was necessary to introduce an additional weakly damaged layer above the bulk material. The four layer fit delivered results for layer thickness d and positron diffusion length L_+ as follows: layer 1: $d = (5 \pm 2)$ nm, $L_+ < 1$ nm; layer 2: $d = (260 \pm 8)$ nm, $L_+ = (10 \pm 1)$ nm; layer 3: $d = (634 \pm 141)$ nm, $L_+ = (49 \pm 14)$ nm. The bulk diffusion length was fixed at $L_+ = 52$ nm.

It is remarkable to note that beside the sample alterations caused by the remote H plasma treatment in the subsurface region (< 1 μ m) the crystal quality of the bulk has clearly undergone further improvement, as indicated by an increase in $L_+ \sim 38$ to ~ 52 nm.

A self-evident explanation could be connected with zinc interstitial (Zn_i) atoms which may exist in the crystal, become mobile at temperatures above ~ 200 °C [30] and may fill up some of existing V_{Zn} -H complexes that were discussed in Ref. [1] to be responsible for positron trapping in HTG ZnO materials. In this case, the original trapping sites are no longer attractive for positrons, which could explain the observed increase of the positron diffusion length.

Another explanation of the observed crystal quality improvement (layers 3 and 4) could be the filling up of V_{Zn} -H complexes by H introduced by the plasma treatment. In the case of $V_{Zn} + 1H$ complexes discussed in Ref. [1] just one additional H atom is enough to fill up the free volume of this defect and make it invisible to positrons.

SPIS results of sample #3 after remote H plasma treatment are shown in Fig. 3 and are comparable to those of sample #2, except for the missing third layer.

An improved approach for the analysis of SPIS data by using a combination of S and W , introduced in a study of the

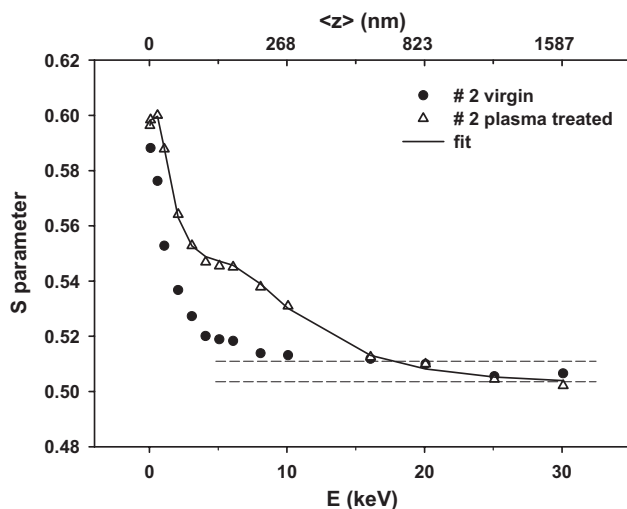


Figure 2 Doppler broadening parameter S of a HTG ZnO single crystal (MT-08, sample #2) in as-received state (polished front side) and after remote H plasma treatment as a function of incident positron energy E . The best fit to the data for the plasma treated sample is given. The mean positron implantation depth $\langle z \rangle$ is given for comparison.

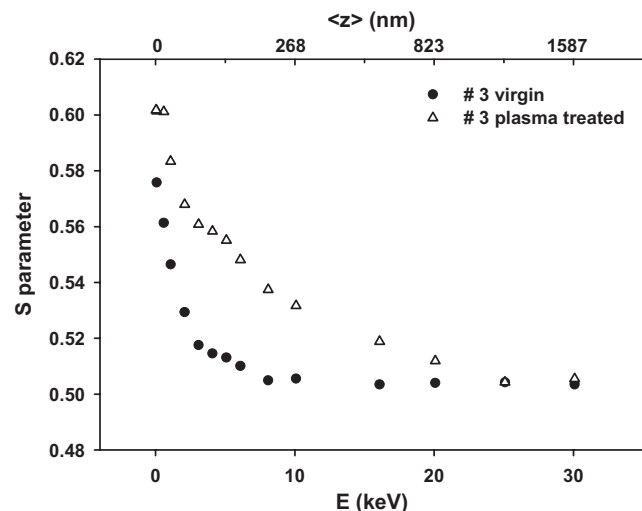


Figure 3 Doppler broadening parameter S of a HTG ZnO single crystal (MT-08, sample #3) in as-received state (polished front side) and after remote H plasma treatment as a function of incident positron energy E . The mean positron implantation depth $\langle z \rangle$ is given for comparison.

SiO₂/Si system [31, 32] and shown to be very useful in a later comprehensive investigation of this system [33], should thus be of interest for the qualitative interpretation of the present SPIS data too. A more recent application of such an *S*–*W* plot regards the formation and stability of rocksalt ZnO nanocrystals in MgO [34] and it can be learned that annihilation in a ZnO crystal and Zn metal both give a comparable value of *W* but a ~13% larger *S* for ZnO. Even anticipating, from the authors' experience [1], that the ZnO crystal which served as a reference in Ref. [34] was not defect-free, the large difference in *S* between ZnO and Zn reported should be beyond any doubt. Therefore, from our present SPIS data it is suggested that the rather high *S* value characterising the narrow subsurface layer of ~260 nm thickness found after the remote H plasma treatment could either indicate enrichment in Zn due to the treatment, or the formation of large open volume defects.

Pulsed low energy positron beam system is complementary to SPIS and has been performed on virgin sample #5 as well as on samples #2 and #3 after remote H plasma treatment. The mean LT (τ_m) values of the three samples are summarized and presented in Fig. 4.

Although the existence of a defected subsurface layer on polished and unpolished sides of virgin ZnO single crystals has already been demonstrated by SPIS [15, 17], its true nature could not be revealed due to the lack of a defect-free ZnO single crystal that might have served as a reference. Regarding the virgin sample #5, the results (Fig. 4) clearly reveal that this damage should consist of very large open volume defects whose depth profile from both sides of the crystal is also evident in the figure.

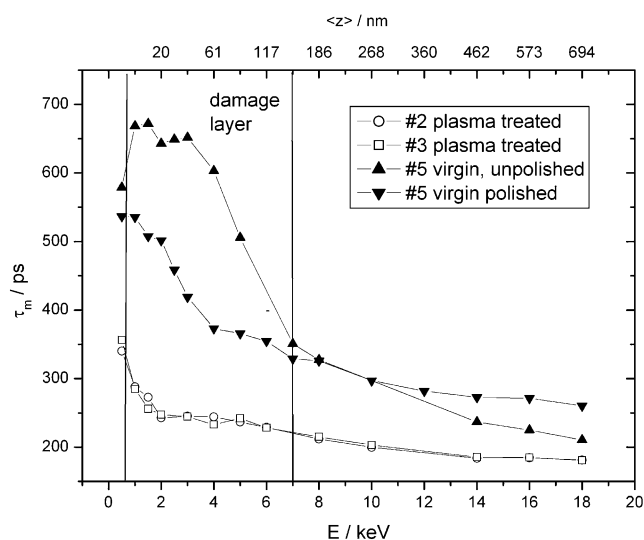


Figure 4 Mean positron lifetime τ_m as a function of incident positron energy *E* in a virgin HTG single crystal (MT-08, sample #5, polished, and unpolished side) and two different HTG ZnO single crystals (MT-08, samples #2 and #3) after remote H plasma treatment. The width of the broad subsurface damage layer found from SPIS (see text) is indicated in terms of corresponding positron energies at which their distribution touches them.

Surprisingly, samples #2 and #3 exhibit a uniform behavior after their remote H plasma treatment. The trend of their mean LTs resembles closely the SPIS data (Figs. 2 and 3). Evidently open volume defects of much smaller size than those detected in the as-received sample are responsible for this trend.

For a more detailed understanding and discussion of the PLEPS results, a mathematical decomposition of all spectra has been performed. Generally, three positron LT components had to be assumed in order to achieve reasonable fitting results.

The longest LT τ_3 of virgin sample #5, samples #2 and #3 after remote H plasma treatment and their corresponding intensities I_3 are shown in Fig. 5.

Generally, τ_3 is found to be of the order 1–3 ns. Such a long LT is usually associated with pick-off annihilations from *ortho*-positronium (*o*-Ps), an atomic-like bound state between an electron and a positron having parallel spin orientation [11, 12]. Correspondingly, *para*-positronium (*p*-Ps) is a bound state of an electron and a positron having anti-parallel spin orientation. Although its intensity is just one third of *o*-Ps its formation can nevertheless influence the measured values of SPIS parameters.

At the virgin sample #5, this longest component shows remarkably high intensities (10% < I_3 < 27%) on both sides of the crystal and is found throughout the subsurface damaged layers as characterized by SPIS. Because this damage depends on the preparation conditions of the crystals by the supplier and cannot be considered to be reproducibly observed, the full decomposition results of the associated PLEPS spectra are not given and discussed here further.

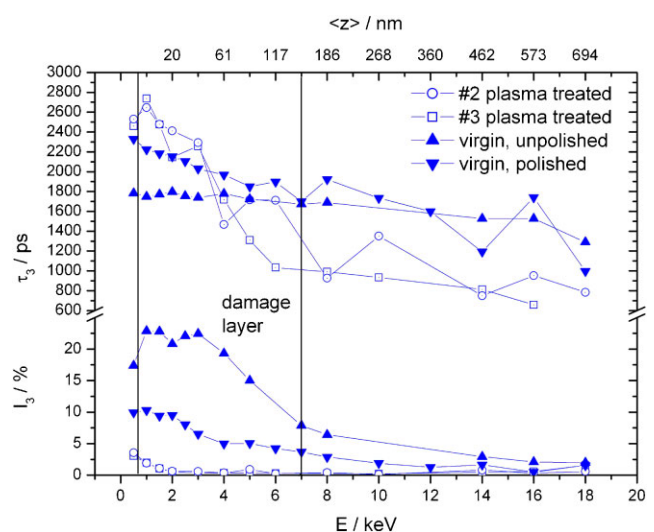


Figure 5 (online color at: www.pss-a.com) Longest positron lifetime τ_3 and corresponding intensity I_3 as a function of incident positron energy *E* in a virgin HTG single crystal (MT-08, sample #5, polished, and unpolished side) and two different HTG ZnO single crystals (MT-08, samples #2 and #3) after remote H plasma treatment. Mean depth $\langle z \rangle$ of positrons is given for comparison.

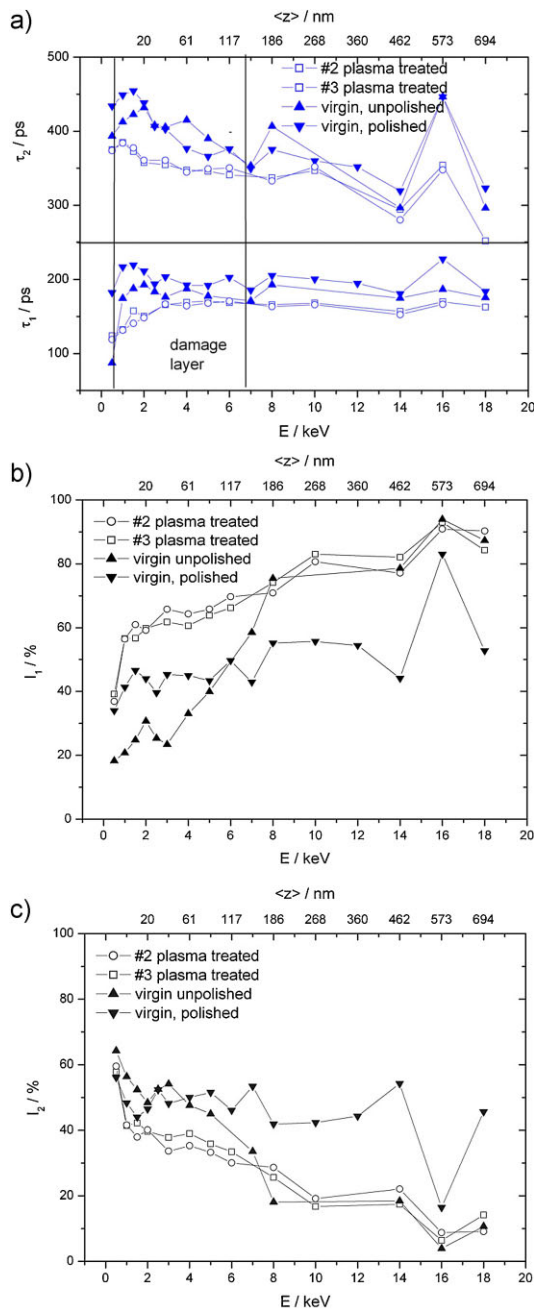


Figure 6 (online color at: www.pss-a.com) (a) Positron lifetimes τ_1 and τ_2 as a function of incident positron energy E for a virgin HTG single crystal (MT-08, sample #5, polished, and unpolished side) and two different HTG ZnO single crystals (MT-08, samples #2 and #3) after remote H plasma treatment. Mean depth $\langle z \rangle$ of positrons is given for comparison. (b) Relative intensity I_1 as a function of incident positron energy E for a virgin HTG single crystal (MT-08, sample #5, polished, and unpolished side) and two different HTG ZnO single crystals (MT-08, samples #2 and #3) after remote H plasma treatment. Mean depth $\langle z \rangle$ of positrons is given for comparison. (c) Relative intensity I_2 as a function of incident positron energy E for a virgin HTG single crystal (MT-08, sample #5, polished, and unpolished side) and two different HTG ZnO single crystals (MT-08, samples #2 and #3) after remote H plasma treatment. Mean depth $\langle z \rangle$ of positrons is given for comparison.

In contrast to that in the virgin sample, the subsurface damage of samples #2 and #3 after remote H plasma treatment is reproducible. It is striking to note that this longest component is almost entirely found near the sample surface with an intensity of $\sim 3\%$ or less. This suggests that it is associated with formation of *o*-Ps at both sample surfaces and identified by SPIS as the very narrow “layer 1” in both crystals, characterized by the very short $L_+ < 1$ nm. The two shorter LT components (τ_1 , τ_2) (Fig. 6a) of samples #2 and #3 after remote H plasma treatment and their corresponding intensities (I_1) (Fig. 6b) and (I_2) (Fig. 6c) are presented in Fig. 6.

As the longest LT component τ_3 of these samples is almost entirely found in “layer 1” the behavior of τ_2 and I_2 is characteristic of annihilation at defects in the subsurface damage “layer 2”. In this layer are mainly seen annihilations from a defect state characterized by a positron LT in the range 350–380 ps, which according to theoretical calculations should correlate with an open volume corresponding to a cluster of four to six (Zn + O) di-vacancies [35]. However, given the complexity of the material, all calculations can only give a rough estimate and do not allow quantitative conclusions about the real size and structure of those defects.

The detailed mechanism of how such large open volume defects of uniform size can form is not known. However, electrochemistry [36] might be useful in finding an explanation as it describes ZnO more generally as a material which due to *structural* disorder exhibits *electronic* disorder. Also, ZnO is known to show thermochromism – i.e. it may change its color reversibly from white to yellow upon heating. This process is accompanied by a loss of oxygen which results in an excess of zinc. The zinc ions will then most probably occupy interstitial lattice positions where they can act as donors having activation energy as low as 0.05 eV. In other words, the amount of free electrons in ZnO is a function of the oxygen partial pressure. Using the law of mass action it is derived that the free carrier concentration n is proportional to the reciprocal fourth root of the oxygen partial pressure [36].

Thus, n-type conductivity will decrease with increasing partial oxygen pressure. An increase of n-type conductivity upon heating of ZnO films up to 450–600 °C which is maintained even up a few days after cooling down to RT has been reported [37]. Another proposed explanation for such an effect is desorption of oxygen atoms at grain boundaries upon heating [38]. These ideas about Zn_i represent one of the views to explain the origin of n-type conductivity of ZnO.

In the case of remote H plasma treatment, however, it can be hypothesized that beside the effect of heating a loss of oxygen is mainly caused by the interaction of ZnO with H at the elevated treatment temperature. If a H ion from the plasma which penetrates the ZnO is trapped into an existing $V_{Zn} + 1H$ defect [1], it forms perhaps a $V_{Zn} + 2H$ complex which does not trap positrons any more [1], or it touches a kind of “inner surface” and it is supposed that it may rip out an oxygen atom from the lattice and form an OH molecule. This molecule might then diffuse towards the crystal surface

and disappear from there by further reactions with the remote H plasma. The $V_{Zn} + 1H$ defects damaged this way could develop into larger open volume defects by repeating this process several times. In contrast, the remaining zinc atoms should be mobile and thus easily diffuse throughout the whole crystal. As mentioned above, this zinc diffusion would cause an increase in n-type conductivity measurable near surface on the one hand but may also result in a filling of $V_{Zn} + 1H$ defects existing in the bulk.

An extended discussion of experimental investigations of the interaction of polar “outer” surfaces of ZnO with either H or O has already been described in the early literature [39], whereas first-principle studies [40, 41] of the diffusion of either V_{Zn} and Zn_i or V_O and O_i in ZnO have been published only recently. If and how such results can be helpful to clarify the mechanism which results in the formation of larger open volume defects of uniform size, as detected here, remains to be discovered from further extensive research.

The formation of nanovoids and nanocolumns in ZnO upon implantation of 100 keV H_2^+ ions with various fluences in the range 5×10^{16} – $3 \times 10^{17} \text{ cm}^{-2}$ and post-implantation annealing up to 800 °C for 1 h has been reported [42]. Exfoliation of a surface layer of ~ 450 nm thickness has been observed in an unusually narrow range of fluences (2.2 – $2.8 \times 10^{17} \text{ cm}^{-2}$). This layer thickness matches well with the projected range of the ions of ~ 400 nm as estimated by SRIM [20]. However, these results are not in favor of a picture that might explain the currently observed void formation by accumulation of excess H atoms in the lattice to form a bubble.

Nanovoid formation upon direct ZnO treatment in H-plasma has been reported elsewhere [43]. From μ -Raman spectroscopy it has been concluded that these nanovoids are created by coalescence of V_O defects and should be filled with H_2 . This finding could be consistent with the following picture: as O atoms go away from the sample during the H plasma treatment, remaining Zn atoms may diffuse away. At the same time, H that is in the neighborhood may help in nucleation of such voids.

It has to be stated, however, that to verify these results [43] by PAS seems to be impossible because V_O defects are not attractive to positrons [1], and in spite of a larger open volume after supposed coalescence still would not be attractive due to their claimed filling with H_2 . On the other hand, in Ref. [43] nothing is mentioned regarding a depth sensitivity of the μ -Raman spectroscopy. Thus, it might be possible that after the direct H plasma treatment near the surface larger open volume defects containing H_2 molecules have been formed. However, according to our results (Fig. 5), only in “layer 1” such a scenario is conceivable after remote plasma but definitely not at greater depth.

Interpretation of results in Ref. [43] relies on PAS studies which report on microvoid formation in hydrogen-implanted HTG ZnO single crystals [44]. It is worth reviewing some of these results now in spite of findings presented in Ref. [1]. The “as-grown” material exhibits a single LT

(182.2 ± 0.7 ps) [45] which should be indicative of saturation trapping in $V_{Zn} + 1H$ defects [1]; however, a box-shaped profile obtained by H^+ implantation with various fluences in the energy range (20–80) keV to achieve a total fluence of $4.4 \times 10^{15} \text{ cm}^{-2}$ is also characterized by a single but slightly larger LT (202.0 ± 0.6 ps) [44] which strongly suggests saturation trapping in V_{Zn} [1]. Post-implantation annealing at 700 °C is found to result in the formation of large empty microvoids which are interpreted as agglomerated V_O defects. Finding of such voids is comparable to the results from Ref. [42] regarding exfoliation. Although hydrogen implantation should generally result in formation of V_{Zn} , Zn_i , V_O , and O_i as basic defects in ZnO, the post-implantation annealing behavior of the damage created by implantation might be influenced in addition by the type of ion (H_2^+ [42], H^+ [44]) used.

To summarize, the mechanism of forming small and evenly distributed open volume defects of a size corresponding to four to six (Zn + O) di-vacancies [35] observed after remote H plasma treatment remains to be determined.

3.2 NRA According to the results from SPIS, an estimate of H concentrations in sample #1 has been performed at two different depths, i.e., 100 and 600 nm, at the polished and unpolished sides. The chosen depth of 100 nm guarantees that volume properties without any influence of surface contamination, and in particular within the first defected layer, are being studied. The second chosen depth (600 nm) allows a judgement of both the third defected layer of sample #2 and the bulk of sample #3 after the remote H plasma treatment. The results are summarized in Table 2.

Figure 7 presents the H concentration at a depth of 100 nm for sample #1 obtained at both the polished and unpolished sides after remote H plasma treatment. At the polished side, a constant value of H-b = (0.58 ± 0.09) at.-%, i.e. $(48.7 \pm 7.6) \times 10^{19} \text{ cm}^{-3}$, is observed. In the virgin sample #1, H-b = (0.14 ± 0.03) at.-%, i.e. $(11.8 \pm 2.5) \times 10^{19} \text{ cm}^{-3}$, has been detected.

When measuring at the unpolished back side of sample #1 at a depth of 100 nm, a decrease of the H content with increasing bombardment by ^{15}N ions is observed which finally reaches a constant level of H-b = (0.64 ± 0.07) at.-%, i.e. $(53.7 \pm 5.9) \times 10^{19} \text{ cm}^{-3}$.

This H-b value is in reasonable agreement with the result obtained at the polished side within the limits of error. From an extrapolation to the yield at the beginning of the ^{15}N bombardment, a concentration of H-u = (2.7 ± 0.9) at.-%,

Table 2 H content H-b (at.-%) of a HTG ZnO single crystal (MT-08, samples no.1) estimated by NRA in different sample states for different depths and sample sides.

sample state	depth = 100 nm	depth = 600 nm	sample side
virgin	0.14 ± 0.03	not measured	polished
H plasma treated	0.58 ± 0.09	0.15 ± 0.03	polished
H plasma treated	0.64 ± 0.07	0.25 ± 0.05	unpolished

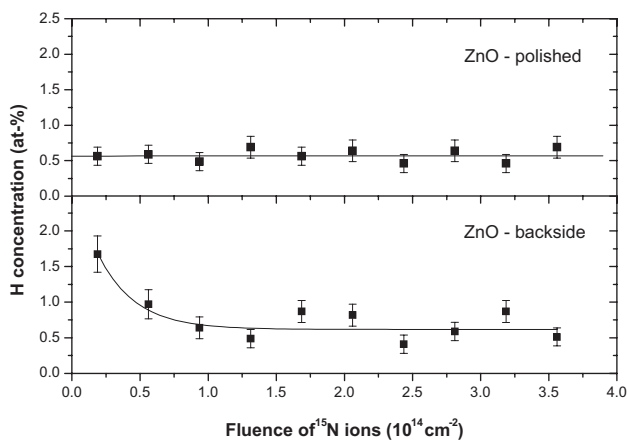


Figure 7 H concentration at 100 nm depth as a function of the sum of ^{15}N ions used for bombardment during NRA analysis of a ZnO single crystal (MT-08) after remote H plasma treatment.

i.e. $(226.7 \pm 75.6) \times 10^{19} \text{ cm}^{-3}$, is derived. The presence of H-u could be due to the fact that the unpolished side is very rough due to lapping. Thus, up to a certain depth from the surface additional extrinsic defects, like dislocations, might exist which could act as sites where this H-u is most probably attached.

When measuring at a depth of 600 nm of sample #1, at the polished side H-b = (0.15 ± 0.03) at.-% is found. This concentration is in excellent agreement with the value of H-b = (0.14 ± 0.03) at.-% estimated for the virgin sample #1 at a depth of 100 nm. This shows that the remote H plasma treatment seemingly does not introduce additional H into the volume of the crystal.

When measuring at a depth of 600 nm of sample #1 at the unpolished side, a value of H-b = (0.25 ± 0.05) at.-% is detected after the remote H plasma treatment, which is a little larger than that found at the polished side in virgin state at 100 nm. This is most probably due to the presence of defects formed as a result of lapping the virgin crystal after cutting from a larger piece by the supplier.

The much smaller H-b value found at 600 nm depth, compared to that at 100 nm, suggests that this is just connected with the additional defects introduced from lapping but also confirms that due to the remote H plasma treatment no additional H is introduced into the volume of the crystal.

At the polished side of sample #1 H-b but no H-u has been observed before and after remote H plasma treatment (Table 2). This is a further strong indication that no H_2 is confined in the evenly distributed open volume defects of a size corresponding to four to six $(\text{Zn} \pm \text{O})$ di-vacancies [35] observed after remote H plasma treatment.

3.3 PAS-LT In contrast to the PAS-SPIS near-surface measurements described in Section 3.2, the measurements discussed in this section reflect volume properties of the ZnO single crystal due to the very large penetration depth of positrons from the ^{22}Na source, see Section 2.3.

The measurement of the five pairs of virgin MT-08 crystals gave an average single positron LT of (180.6 ± 0.5) ps, which is ~ 1 ps less than the average number of (181.7 ± 0.3) ps measured in the previously studied MT-06 series [1] but again well above a derived bulk LT of $\tau_b = (151 \pm 2)$ ps [17].

After the remote H plasma treatment, sample #1 exhibits a two component LT spectrum as follows: $\tau_1 = (50 \pm 10)$ ps, $I_1 = (6 \pm 1) \%$, $\tau_2 = (175.9 \pm 0.5)$ ps, and $I_2 = (94 \pm 1) \%$. No constraints to the fit have been applied. The application of the two-state trapping model [11, 12] gives a bulk LT of $\tau_b = (153 \pm 2)$ ps, in very good agreement with a previously derived value of $\tau_b = (151 \pm 2)$ ps [17]. This result is remarkable for three reasons, because (1) a free positron component appears in the LT spectrum, i.e., no more saturation trapping occurs, (2) a slight drop in the τ_2 value compared to the originally measured 180.6 ps is observed, and (3) at the same time the NRA results did not indicate additional introduction of H into the volume of the crystal.

The appearance of a LT component indicating the annihilation of free positrons in the ZnO bulk can only be due to a reduction of the defect concentration which originally caused saturation trapping. As a $\text{V}_{\text{Zn}} \pm 1\text{H}$ complex has been supposed [1] to be responsible for the saturation trapping throughout the volume of the HTG crystals, this complex can become invisible to positrons in two ways: (1) by conversion into $\text{V}_{\text{Zn}} \pm n\text{H}$ complexes with $n > 2$ which are found to not trap positrons any more [1], or (2) by filling with a Zn_i atom. Case (1) most probably happens within a subsurface depth of less than ~ 600 nm, whereas case (2) certainly must happen throughout the crystal volume.

The presence of Zn_i in the virgin crystal is reliably concluded from PL and Hall measurements – these results are reported and discussed in the second part of this paper [45]. Unfortunately, no estimate concerning the Zn_i concentration can be derived from these measurements. As discussed above, the creation of further Zn_i is expected from the remote H plasma treatment but not all results published in the literature (see, e.g., Ref. [46]) fully support this idea. However, case (2) is well supported by SPIS considering the bulk diffusion length $L_+ \sim 38$ nm in the as-received state and its increase to ~ 52 nm after the treatment, and also because Zn_i become mobile at temperatures above $\sim 200^\circ\text{C}$ [30]. This explanation is also in agreement with the PAS-LT sensitivity regarding depth – see Chapter 2.3.

The macroscopic effects of the remote plasma treatment on the ZnO crystals are expected to be manifold: (1) excess O or water molecules are removed from the crystal surface by a reaction with the H from the plasma, (2) the plasma simultaneously prevents the take-up of O from the ambient atmosphere, and (3) a surface layer of super-stoichiometric zinc atoms is formed which act as donors with rather low activation energy [30]. The last effect is directly confirmed by our Hall results, see Ref. [45].

Any certain explanation of the experimentally observed drop of 4.7 ps in the defect LT due to the remote plasma treatment is neither obvious nor straightforward. A structural

modification of the remaining $V_{Zn} \pm 1H$ complexes could have happened which results in a reduction of their open volume seen in the slight drop of the defect LT. Similarly, such a slight drop (of ~ 3 ps) has already been observed in connection with electrochemical H loading of a HTG ZnO single crystal (MT-06) [3], although in this case much more H has been introduced into the volume of the crystals and, at the same time, no free positron LT component was observed.

For the purpose of comparison and in order to clarify the possible role of annealing temperature on the observed slight drop in positron LT, another ZnO sample pair (#7 \pm #8) was just treated at 350 °C for 1 h in air. This resulted in a smaller drop of the positron LT from (180.4 ± 0.4) to (177.9 ± 0.2) ps compared to the drop observed at sample pair (#2 \pm #3) after treatment in H plasma at comparable temperature and time, but without the appearance of a second LT.

A similar small drop has been observed previously [1] for the HTG sample pair (#5 \pm #6) where annealing in air at 500 °C for 30 min resulted in a shift from (181.2 ± 0.3) to (179.7 ± 0.4) ps without occurrence of a second positron LT. Annealing in air is not expected to be connected with a drastic loss in O with the creation of additional Zn_i in the ZnO crystals comparable to remote H plasma treatment. However, O could now be adsorbed on the surface and then Zn_i atoms may be moving towards the surface [30], filling up some positron trapping sites on their way. Therefore, the lack of a second positron LT after such a treatment can more or less be understood.

In the case of electrochemically H-loaded ZnO samples [3], there is a gradual decrease of the positron LT with increasing H content, but the remote H plasma treatment applied in this investigation causes a noticeably larger decrease in the positron LT than that due to annealing in air at 350 °C (Fig. 8).

This suggests that the LT decrease observed in electrochemically loaded and remote H plasma treated samples is

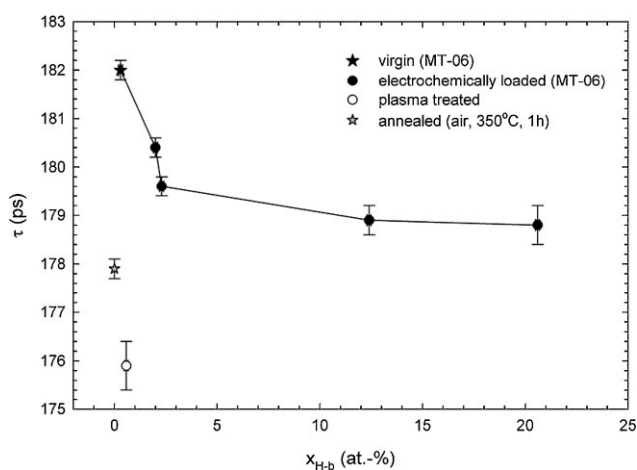


Figure 8 Positron lifetime τ of differently treated HTG ZnO single crystals as a function of their bound H content x_{H-b} .

different in origin. To find the true nature of the structural effect causing this drop in LT remains a real challenge for further studies.

3.4 PAS – Relation to other experimental data In Ref. [1] we have given an extensive summary of literature regarding positron annihilation studies of ZnO.

One comment concerns irradiated ZnO samples studied using LT [47] where several samples (both HTG and MG) exhibited a LT component corresponding to delocalized positrons after electron irradiation – like in the present study after remote H plasma treatment – even if the non-irradiated samples did not show such a component. It should be mentioned that our very first (yet unpublished) results for HTG ZnO (MT-06) samples irradiated by 10 MeV electrons at RT indicate a similar behavior. In both cases of irradiation it is difficult to speculate about the origin of the observed effect because Zn_i and O_i atoms are created during electron irradiation, but at the same time V_{Zn} and V_O are also produced. To elucidate which process could lead to a filling of open volume defects present before irradiation, so that a LT component corresponding to delocalized positrons is observed, remains a challenge for further investigations.

Li impurities are often considered in relation to defects in ZnO. In two recent works [48, 49] gettering of Li impurities by V_{Zn} clusters is observed. However, theoretical results for the $V_{Zn} + Li$ complex from Ref. [1] have shown that this defect most probably does not constitute a positron trap [1]. This means that in Ref. [48] another, more complex defect involving V_{Zn} has to be responsible for the observed effects. In any case, Li related effects cannot explain our bulk PAS results because (i) the presence of Li in our samples, if any, is rather low and not enhanced by corresponding ion implantation as in Ref. [48], (ii) our samples undergo a heat treatment at 350 °C for 1 h during the remote H plasma treatment, and (iii) gettering, if it occurs in our samples, might be expected only in the ~ 260 nm layer modified by the H plasma treatment and definitely not in the bulk of the crystal. Also, it was reported in Ref. [49] that nitrogen implantation into ZnO results in the formation of clusters containing two to four V_{Zn} 's which getter Li impurities. But the same arguments also hold for this case, and similar effects cannot influence interpretation of our PAS data.

4 Conclusions An extended investigation of HTG ZnO single crystals, before and after treatment in remote H plasma, has been performed by PAS (SPIS, PLEPS, LT) measurements. The H content before and after the H plasma treatment has been determined using NRA.

A varying quality of crystal polishing from the same supplier has been noticed over the years. On the other hand, the bulk quality has improved – reflected by an increase in the measured positron diffusion length from (22 ± 1) nm previously to (38 ± 11) nm now. An average single positron LT of (180.6 ± 0.5) ps is consistently measured for five pairs of virgin crystals, which is ~ 1 ps less than the average value of (181.7 ± 0.3) ps measured by the authors for a previous

sample set but well above an earlier derived bulk LT of $\tau_b = (151 \pm 2)$ ps [17].

An explanation of the experimentally observed drop of 4.7 ps in the defect LT due to the remote plasma treatment cannot be given and remains to be determined. From the observed appearance of a LT component indicating the annihilation of free positrons in bulk ZnO a positron bulk LT of $\tau_b = (153 \pm 2)$ ps could be derived, in very good agreement with the value referred to above.

As Li impurities are often considered in relation to defects in ZnO, it has been noted that Li related effects cannot explain our bulk PAS results and thus cannot influence interpretation of our PAS data.

In a second part of this work, complementary temperature-dependent Hall (TDH) measurements for electrical characterization and supplementary PL studies have been performed on HTG ZnO single crystals, before and after treatment in remote H plasma, and an extensive discussion of the modification of electrical and optoelectronic properties is presented [45].

Acknowledgements We are thankful to F. Börrnert (TU Dresden) for his careful treatment of the ZnO samples in remote H plasma. We would like to thank G. Kögel (UBW Neubiberg) for helpful discussions in the interpretation of the PLEPS lifetime data. This work is part of the research plan MS 0021620834 and project no. COST OC 165 that are financed by the Ministry of Education of the Czech Republic. Support of the Grant Agency of the Academy of Sciences of the Czech Republic under the project no. KJB101120906 is also acknowledged.

References

- [1] G. Brauer, W. Anwand, D. Grambole, J. Grenzer, W. Skorupa, J. Cizek, J. Kuriplach, I. Prochazka, C. C. Ling, C. K. So, D. Schulz, and D. Klimm, *Phys. Rev. B* **79**, 115212 (2009).
- [2] J. Kuriplach, G. Brauer, O. Melikhova, J. Cizek, I. Prochazka, and W. Anwand, in: *Zinc Oxide and Related Materials – 2009*, edited by S. Durbin, M. Allen, and H. von Wenckstern, Mater. Res. Soc. Symp. Proc., Vol. 1201 (Materials Research Society, Warrendale, PA, 1201-H02-03, 2010).
- [3] J. Cizek, N. Zaludova, M. Vlach, S. Danis, J. Kuriplach, I. Procházka, G. Brauer, W. Anwand, D. Grambole, W. Skorupa, R. Gemma, R. Kirchheim, and A. Pundt, *J. Appl. Phys.* **103**, 053508 (2008).
- [4] Y. M. Strzhemechny, J. Nemergut, P. E. Smith, J. Bae, D. C. Look, and L. J. Brillson, *J. Appl. Phys.* **94**, 4256 (2003).
- [5] Y. M. Strzhemechny, H. L. Mosbacker, D. C. Look, D. C. Reynolds, C. W. Litton, N. Y. Garces, N. C. Giles, and L. E. Halliburton, *Appl. Phys. Lett.* **84**, 2545 (2004).
- [6] Y. M. Strzhemechny, H. L. Mosbacker, S. H. Goss, D. C. Look, D. C. Reynolds, C. W. Litton, N. Y. Garces, N. C. Giles, L. E. Halliburton, S. Niki, and L. J. Brillson, *J. Electron. Mater.* **34**, 399 (2005).
- [7] C. G. Van de Walle, *Phys. Rev. Lett.* **85**, 1012 (2000).
- [8] A. Janotti and C. G. Van de Walle, *Nat. Mater.* **6**, 44 (2007).
- [9] A. Eicke and G. Bilger, *Fresenius J. Anal. Chem.* **341**, 214 (1991).
- [10] F. Pavlyak, *Surf. Interface Anal.* **19**, 232 (2004).
- [11] A. Dupasquier and A. P. Mills, Jr. (Eds.), *Positron Spectroscopy of Solids* (IOS, Amsterdam, 1995).
- [12] R. Krause-Rehberg and H. S. Leipner, *Positron Annihilation in Semiconductors – Defect Studies* (Springer, Berlin, 1999).
- [13] G. Brauer and W. Anwand (Eds.), *Proceedings of the Ninth International Workshop on Slow-Positron Beam Techniques for Solids and Surfaces*, Dresden, 2001.
- [14] W. Bauer-Kugelmann, P. Sperr, G. Kögel, and W. Triftshäuser, *Mater. Sci. Forum* **363-365**, 529 (2001).
- [15] G. Brauer, W. Anwand, W. Skorupa, J. Kuriplach, O. Melikhova, J. Cizek, I. Prochazka, C. Moisson, H. von Wenckstern, H. Schmidt, M. Lorenz, and M. Grundmann, *Superlattices Microstruct.* **42**, 259 (2007).
- [16] E. H. Kisi and M. M. Elcombe, *Acta Crystallogr. C* **45**, 1867 (1989).
- [17] G. Brauer, W. Anwand, W. Skorupa, J. Kuriplach, O. Melikhova, C. Moisson, H. von Wenckstern, H. Schmidt, M. Lorenz, and M. Grundmann, *Phys. Rev. B* **74**, 045208 (2006).
- [18] W. A. Lanford, *Nuclear Reactions for H Analysis*, in: *Handbook of Modern Ion Beam Materials Analysis*, edited by R. Tesmer and M. Nastasi (Materials Research Society, Pittsburgh/PA, 1995), p. 193.
- [19] G. Brauer, W. Anwand, D. Grambole, W. Skorupa, Y. Hou, A. Andreev, C. Teichert, K. H. Tam, and A. B. Djuricic, *Nanotechnology* **18**, 195301 (2007).
- [20] J. F. Ziegler, J. P. Biersack, and U. Littmark, *The Stopping and Range of Ions in Solids* (Pergamon, New York, 1985).
- [21] W. Anwand, H.-R. Kissener, and G. Brauer, *Acta Phys. Pol. A* **88**, 7 (1995).
- [22] A. van Veen, H. Schut, J. de Vries, R. A. Hakvoort, and M. R. Ijpma, in: *Positron Beams for Solids and Surfaces*, edited by P. J. Schultz, G. R. Massoumi, and P. J. Simpson (American Institute of Physics, New York, 1990), p. 171.
- [23] W. Egger, P. Sperr, G. Kögel, and G. Dollinger, *Phys. Status Solidi C* **4**, 3969 (2007).
- [24] P. Sperr, W. Egger, G. Kögel, G. Dollinger, C. Hugenschmidt, R. Repper, and C. Piochacz, *Appl. Surf. Sci.* **255**, 35 (2008).
- [25] R. I. Grynszpan, W. Anwand, G. Brauer, and P. G. Coleman, *Ann. Chim. Sci. Mater.* **32**, 365 (2007).
- [26] F. Becvar, J. Cizek, L. Lestak, I. Novotny, I. Prochazka, and F. Sebesta, *Nucl. Instrum. Methods A* **443**, 557 (2000).
- [27] I. Prochazka, I. Novotny, and F. Becvar, *Mater. Sci. Forum* **255-257**, 772 (1997).
- [28] H. von Wenckstern, H. Schmidt, C. Hanisch, M. Brandt, C. Czekalla, G. Benndorf, G. Biehne, A. Rahm, H. Hochmuth, M. Lorenz, and M. Grundmann, *Phys. Status Solidi RRL* **1**, 129 (2007).
- [29] S. Graubner, C. Neumann, N. Volbers, B. K. Meyer, J. Bläsing, and A. Krost, *Appl. Phys. Lett.* **90**, 042103 (2007).
- [30] R. A. Rabadanov, M. K. Gusekhanov, I. Sh. Aliev, and S. A. Semilov, *Izv. Vys. Ucheb. Zaved., Fiz.* **6**, 72 (1981).
- [31] M. Clement, J. M. M. De Nijs, A. van Veen, H. Schut, and P. Balk, *J. Appl. Phys.* **79**, 9029 (1996).
- [32] M. Clement, J. M. M. De Nijs, A. Van Veen, H. Schut, and P. Balk, *IEEE Trans. Nucl. Sci.* **42**, 1717 (1995).
- [33] G. Brauer, W. Anwand, W. Skorupa, A. G. Revesz, and J. Kuriplach, *Phys. Rev. B* **66**, 195331 (2002).
- [34] S. W. H. Eijt, J. de Roode, H. Schut, B. J. Kooi, and J. Th. M. De Hosson, *Appl. Phys. Lett.* **91**, 201906 (2007).

- [35] Z. Q. Chen, M. Maekawa, S. Yamamoto, A. Kawasuso, X. L. Yuan, T. Sekiguchi, R. Suzuki, and T. Ohdaira, *Phys. Rev. B* **69**, 035210 (2004).
- [36] H. Rickert, *Electrochemistry of Solids* (Springer, Berlin, 1982).
- [37] D. Bao, H. Gu, and A. Kuang, *Thin Solid Films* **312**, 37 (1998).
- [38] P. Nunes, B. Fernandes, E. Fortunato, P. Vilarinho, and R. Martins, *Thin Solid Films* **337**, 176 (1999).
- [39] G. Heiland and P. Kunstmann, *Surf. Sci.* **13**, 72 (1969).
- [40] G.-Y. Huang, C.-Y. Wang, and J.-T. Wang, *Solid State Commun.* **149**, 199 (2009).
- [41] G.-Y. Huang, C.-Y. Wang, and J.-T. Wang, *J. Phys.: Condens. Matter* **21**, 195403 (2009).
- [42] R. Singh, R. Scholz, U. Gösele, and S. H. Christiansen, in: *Zinc Oxide and Related Materials*, edited by J. Christen, C. Jagadish, D. C. Look, and T. Yao, *MRS Symp. Proc.* **957**, 0957-K09-01 (2007) (Materials Research Society, Warrendale/PA).
- [43] R. Job, in: *Semiconductor Defect Engineering – Materials, Synthetic Structures and Devices II*, edited by S. Ashok, P. Kiesel, J. Chevallier, and T. Ogino, *MRS Symp. Proc.* **994**, 0994-F02-09 (2007) (Materials Research Society, Warrendale/PA).
- [44] Z. Q. Chen, A. Kawasuso, Y. Xu, H. Naramoto, X. L. Yuan, T. Sekiguchi, R. Suzuki, and T. Ohdaira, *Phys. Rev. B* **71**, 115213 (2005).
- [45] W. Anwand, G. Brauer, T. E. Cowan, V. Heera, H. Schmidt, W. Skorupa, H. von Wenckstern, M. Brandt, G. Benndorf, and M. Grundmann, *Phys. Status Solidi A* **207**, 2426 (2010), this issue.
- [46] F. A. Selim, M. H. Weber, D. Solodovnikov, and K. G. Lynn, *Phys. Rev. Lett.* **99**, 085502 (2007).
- [47] S. Brunner, W. Puff, A. G. Balogh, and P. Mascher, *Mater. Sci. Forum* **363-365**, 141 (2001).
- [48] T. M. Børseth, F. Tuomisto, J. S. Christensen, W. Skorupa, E. V. Monakhov, B. G. Svensson, and A. Y. Kuznetsov, *Phys. Rev. B* **74**, 161202 (R) (2006).
- [49] T. M. Børseth, F. Tuomisto, J. S. Christensen, E. V. Monakhov, B. G. Svensson, and A. Y. Kuznetsov, *Phys. Rev. B* **77**, 045204 (2008).